Experimental investigation of rheological behavior of the hybrid nanofluid of MWCNT–alumina/water (80%)–ethylene-glycol (20%)

Ashkan Afshari, Mohammad Akbari, Davood Toghraie & Mohammad Eftekhari Yazdi

Journal of Thermal Analysis and Calorimetry
An International Forum for Thermal Studies

ISSN 1388-6150
Volume 132
Number 2

J Therm Anal Calorim (2018)
132:1001-1015
DOI 10.1007/s10973-018-7009-1

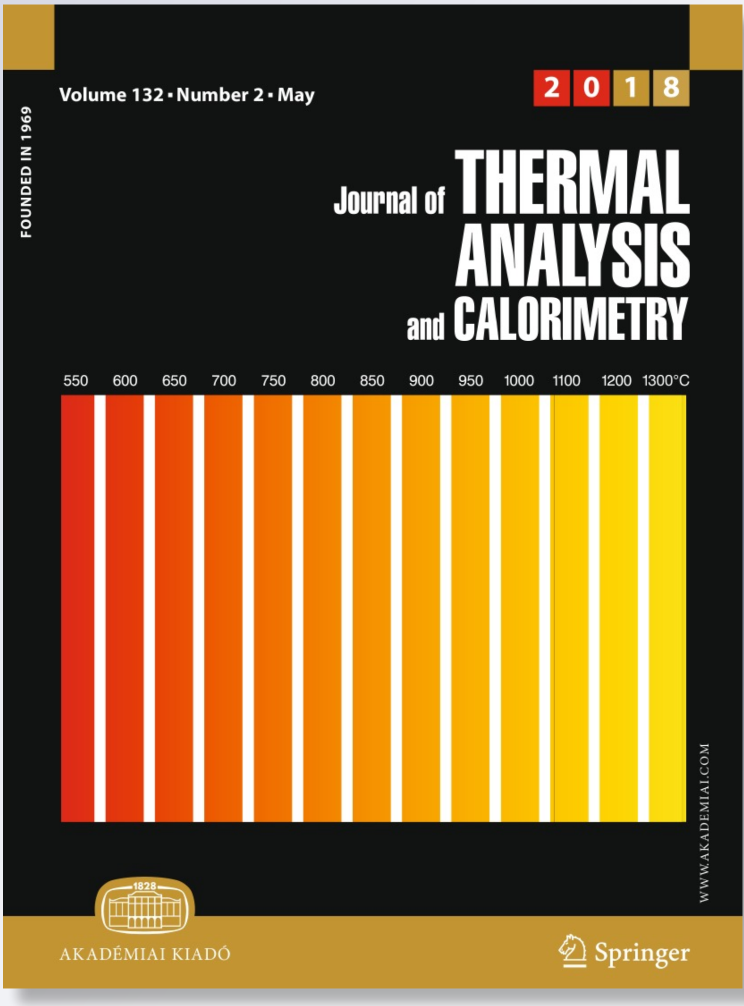

Springer

Journal of Thermal Analysis and Calorimetry (2018) 132:1001–1015
https://doi.org/10.1007/s10973-018-7009-1

Experimental investigation of rheological behavior of the hybrid nanofluid of MWCNT–alumina/water (80%)–ethylene-glycol (20%)

New correlation and margin of deviation

Ashkan Afshari[1] · Mohammad Akbari[2] · Davood Toghraie[3] · Mohammad Eftekhari Yazdi[1]

Received: 29 October 2017 / Accepted: 15 January 2018 / Published online: 2 February 2018

Abstract

Nanofluids are prepared by suspending the nanoparticles in the base fluid and can be substantially enhanced the heat transfer rate compared to the pure fluids. In this paper, experimental investigation of the effects of volume concentration and temperature on dynamic viscosity of the hybrid nanofluid of multi-walled carbon nanotubes and aluminum oxide in a mixture of water (80%) and ethylene-glycol (20%) has been presented. The nanofluid was prepared with solid volume fractions between 0.0625 and 1%, and experiments were performed in the temperature range of 25–50 °C. The measurement results at different shear rates showed that the base fluid and nanofluid samples with solid volume fractions of less than 0.5% had Newtonian behavior, while those with higher solid volume fractions (0.75 and 1%) exhibit a pseudoplastic rheological behavior with a power law index of less than unity. The results showed that viscosity has a direct relationship with solid volume fraction of the nanofluid. The value of maximum enhancement is which occurred in 25 °C. Moreover, the consistency index and power law index have been obtained by accurate curve fitting for samples with non-Newtonian behavior of nanofluids. The results also revealed that the apparent viscosity generally increases with an increase in the solid volume fraction.

Keywords Viscosity · Non-Newtonian behavior · Nanofluids · Aluminum oxide · Multi-walled carbon nanotubes

List of symbols

d	Diameter (nm)
m	Mass (kg)
T	Temperature (°C)

Greek letters

ϕ	Solid volume fraction (%)
γ	Shear rate (s^{-1})
μ	Dynamic viscosity (kg m^{-1} s^{-1})
ρ	Density (kg m^{-3})
τ	Shear stress (mPa)

✉ Mohammad Akbari
m.akbari.g80@gmail.com

1 Department of Mechanical Engineering, School of Engineering, Central Tehran Branch, Islamic Azad University, Tehran, Iran

2 Department of Mechanical Engineering, Najafabad Branch, Islamic Azad University, Najafabad, Iran

3 Department of Mechanical Engineering, Khomeinishahr Branch, Islamic Azad University, Khomeinishahr, Iran

Subscripts

bf	Base fluid
Exp	Experimental data
nf	Nanofluid
Pred	Predicted value
MWCNT	Multi walled carbon nanotubes
Al_2O_3	Alumina
EG	Ethylene glycol

Introduction

A mixture of water and ethylene glycol (EG), called antifreeze coolant, is used for application in cooling systems, heat exchangers, solar collectors, automobile radiators and so on.

Nanofluids are colloids made of nanoparticles suspended in a base fluid. During the past decade, many researches are mostly focused on thermal conductivity of nanofluids and its applications [1–17]. However, nanofluid's viscosity is as important as thermal conductivity in thermal application involving fluid flow.

Namburu et al. [18] studied viscosity of copper oxide nanoparticles dispersed in ethylene-glycol and water mixture. They developed an experimental correlation based on the data, and related viscosity with particle volume percent and the nanofluid temperature.

Chen et al. [19] investigated rheological behavior of nanofluids. They found that the shear thinning behavior of nanofluids depends on the effective particle concentration, the range of shear rate and viscosity of the base liquid. Chen et al. [20] investigated rheological behavior of nanofluids containing Titanate nanotubes nanoparticles. Their results show a very strong shear thinning behavior of the Titanate nanotubes nanofluids and big influences of particle concentration and temperature. Masoumi et al. [21] presented a new model for calculating the effective viscosity of nanofluids. They compared predicted results with other published experimental results for different nanofluids and observed very good concordance between these results. Fedele et al. [22] measured viscosity and thermal conductivity of water-based nanofluids containing titanium oxide nanoparticles. They concluded that the nanofluid at 1 wt.% shows a water-like behavior, but at the higher concentrations the viscosity enhancement is not proportional and surprising excessive. Mahbubul et al. [23] investigated the viscosity of R123–TiO_2 nanorefrigerant. They found that viscosity of nanorefrigerant increased accordingly with the increase in nanoparticle volume concentrations and decreases with the increment of temperature. Mishra et al. [24] reviewed viscosity of nanofluids. They investigated the effects of shape and size, temperature, volume concentration and pH of nanoparticles. Anoop et al. [25] studied the rheology of mineral oil–SiO_2 nanofluids at high pressure and high temperatures. They found that the viscosity values of nanofluid and the base fluid increased as the pressure increased. Also, the nanofluid exhibits non-Newtonian behavior at high temperatures and pressures. Nwosu et al. [26] investigated nanofluid viscosity models. They observed inconsistencies in the model formulations and the predicted data. Li et al. [27] investigated rheological behavior of ethylene-glycol-based SiC nanofluids. They concluded that viscosity of the studied nanofluids increased with volume fractions but decreased with temperatures. Ghozatloo et al. [28] investigated the nanoparticles morphology on viscosity of nanofluids. They concluded that, the viscosity of nanofluids increases with increasing of nanoparticle volume fraction. Etaig et al. [29] investigated the new effective viscosity model for nanofluids. Their simulations show that the effective viscosity model increases with the increase in the volume fraction. Issa [30] studied the effect of nanoparticles size and concentration on thermal and rheological properties of Al_2O_3–water nanofluids. He found that Al_2O_3–water nanofluids viscosity increases with the increase in the suspensions concentration. Auriemma and Iazzetta [31] modeled viscosity of Al_2O_3–water-based nanofluids by artificial neural network (ANN). They compared viscosity results ANN with the experimental data points. Kavosh [32] studied the viscosity of CuO nanofluid based on propylene glycol. He showed that there is a decrease in viscosity of this nanofluid with increase in nanoparticles concentration. Zhao and Li [33] predicted viscosity of different ethylene-glycol/water-based nanofluids by using of a radial basis function Neural Network.

Hemmat Esfe [34] investigated the effects of temperature and nanoparticles volume fraction on the viscosity of copper oxide–ethylene-glycol nanofluids. He found that in a given volume fraction when temperature increases, viscosity decreases, but relative viscosity varies.

In this paper, the dynamics viscosity of hybrid nanofluid of multi-walled carbon nanotubes (MWCNTs) and aluminum oxide (Al_2O_3) in a mixture of water (80%) and ethylene-glycol (20%) is examined experimentally. To the author's knowledge, there is no comprehensive and thorough investigation to predict the dynamics viscosity of the supposed nanofluid.

Preparation of nanofluid

Material preparation and specifications

The first stage of conducting experiments on nanofluids is to prepare the nanofluid. For more precise experiments, the nanofluid should be stable and homogeneous; that is, if the prepared nanofluid is stagnant for a while, sedimentation must not occur. In this study, two-stage method was used to prepare nanofluid. First of all, Al_2O_3 in a mixture of water (80%) and ethylene-glycol (20%) in the range 0.0625% to 1% was prepared by mixing dry samples of MWCNTs and

Table 1 Specifications of MWCNTs and Al_2O_3 nanoparticles

Specifications	Value	
	MWCNTs	Al_2O_3
Purity/%	> 97	> 99
Color	Black	White
Size/nm	Outer diameter = 5–15	20
	Inner diameter = 3–5	
	Length = 50 μm	
Thermal conductivity/W m^{-1} k^{-1}	1500	30
Density/g cm^{-3}	~ 2.1	3.89
Specific surface/m^2 g^{-1}	> 233	> 138

Table 2 Specifications of water and ethylene-glycol

Specifications	Value	
	Ethylene-glycol	Water
Molar mass/g mol^{-1}	62.07	18.02
Appearance	Colorless transparent liquid	Almost colorless transparent
Smell	Smell-less	Smell-less
Density/kg m^{-3}	1113.20	998.21
Melting point/°C	− 12.9	0.00
Boiling point/°C	197.3	100
Thermal conductivity/W m^{-1} k^{-1}	0.224 in 20 °C	0.6 in 20 °C
Viscosity/cP	16.1 in 20 °C	1 in 20 °C

Al_2O_3 nanoparticles (50:50) in a certain amount of a dual mixture of water and ethylene-glycol (20:80). Tables 1 and 2 show the specifications of MWCNTs and Al_2O_3 nanoparticles and the specifications of water and ethylene-glycol that are used in the experiments. The above nanofluid which consists of MWCNTs and Al_2O_3 nanoparticles and water–ethylene-glycol is injected into a 600-ml beaker. The solution was then mixed with magnetic stirrer for 2 h and eventually aggregates particles breakdown operation, and complete dissolution of nanoparticles in base fluid is occurred by ultrasonic process (Hielscher, Germany) with a 400-W power and a frequency of 24 kHz for 6 h. Dynamics viscosity of hybrid nanofluid of multi-walled carbon nanotubes (MWCNTs) and aluminum oxide (Al_2O_3) in a mixture of water (80%) and ethylene-glycol (20%) are measured using the DV-I PRIME Brookfield digital viscometer which has a double-wall cylindrical container. It should be noted that in order to measure the viscosity of low-volume liquids in UL Adaptor at different temperatures and temperature adjustments, it is necessary to have a bath of water. The temperatures used in this study are 25, 30, 35, 40, 45, 50 °C. The water temperature was brought up to 50 °C, and then the water is pumped back and forth into the UL Adapter unit. For lower temperatures also the water temperature in the water bath is brought to the desired temperature. After water temperature reached the required temperature for the test, the nanofluid is poured into the UL Adapter and the test is carried out at various temperatures by using of a Brookfield Viscometer. In order to ensure the structure of nanoparticles and their size, dry samples of MWCNTs and Al_2O_3 nanoparticles were tested using X-ray diffraction method. The size of the nanoparticles and their structure were proven by the XRD diagram. The XRD diagrams of nanotubes and nanoparticles are shown in Figs. 1 and 2. Also, samples of nanoparticles and nanotubes are shown in Fig. 3.

Also, the required value of MWCNTs and Al_2O_3 nanoparticles in different volume fractions can be calculated using Eq. (1), where φ is volume fraction, ρ is density, and m is mass.

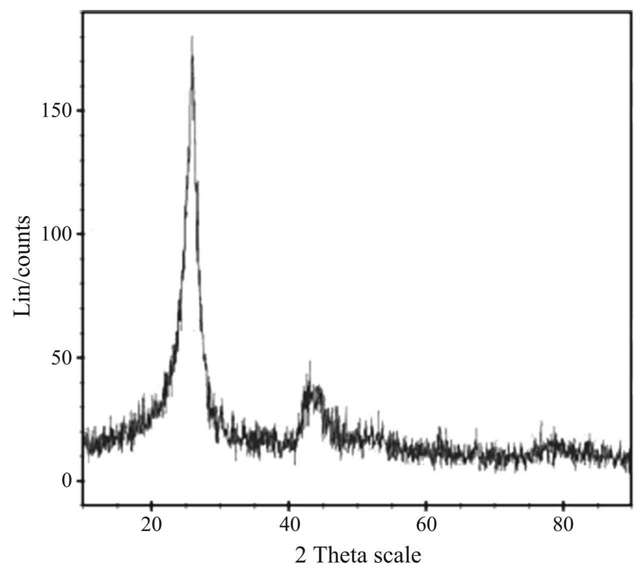

Fig. 1 XRD image of multi-walled carbon nanotubes nanoparticle

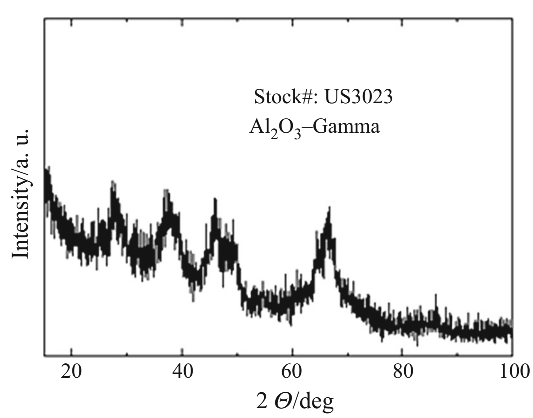

Fig. 2 XRD image of aluminum oxide nanoparticle

$$\varphi = \left[\frac{\left(\frac{M}{\rho}\right)_{Al_2O_3} + \left(\frac{M}{\rho}\right)_{MWCNTs}}{\left(\frac{M}{\rho}\right)_{Water} + \left(\frac{M}{\rho}\right)_{EG} + \left(\frac{M}{\rho}\right)_{Al_2O_3} + \left(\frac{M}{\rho}\right)_{MWCNTs}} \right] \times 100 \quad (1)$$

Fig. 3 Nanoparticles of nanotubes (right), aluminum oxide nanoparticles (left)

Table 3 shows the required value of MWCNTs and Al_2O_3 nanoparticles in different volume fractions.

Measurement of the viscosity

In this experiment, before measuring the dynamic viscosity of the nanofluid, the viscometer was tested with ethylene-glycol and water at room temperature. Also, in order to investigate the rheological behavior (Newtonian or non-Newtonian) of the nanofluid, all experiments were repeated at different shear rates for each volume fraction and

Table 3 Required value of multi-walled carbon nanotubes and aluminum oxide nanoparticles in different volume fractions

No.	Volume fraction/%	Density/g cm^{-3}		Mass/g	
		Al_2O_3	MWCNT	Al_2O_3	MWCNT
1	1	3.89	2.1	11.67	6.3
2	0.75			8.75	4.72
3	0.5			5.83	3.15
4	0.25			2.91	1.57
5	0.125			1.45	0.78
6	0.0625			0.729	0.39

Table 4 A sample of measurements in a volume fraction of 0.25% and a temperature of 35 °C

Volume fraction/%	Temperature/°C	rpm	Viscosity/cP	Shear rate/s^{-1}	Shear stress/Pa
35	0.25	20	1.68	24.46	0.0410
		30	1.64	36.69	0.0601
		40	1.62	48.92	0.07925
		50	1.58	61.15	0.096617
		60	1.56	73.38	0.0114472

Table 5 The values of the whole range and error

	Volume fraction/%	Temperature/°C	rpm	Whole range/cP	Error
1	0.0625	25	20	1.6	0.3159
2			20	1.59	0.2158
3			20	1.58	0.1657
4			20	1.56	0.1355
5			20	1.54	0.1153

Table 6 The rheological behavior of the base fluid at 25 °C

Temperature/°C	Shear rate		Viscosity		Shear stress/dyne cm^{-2}
	rpm	s^{-1}	cP	Poise	
25	20	24.46	1.51	0.0151	0.3693
	30	36.69	1.51	0.0151	0.5503
	40	48.92	1.49	0.0149	0.7289
	50	61.15	1.47	0.0147	0.8989
	60	73.38	1.45	0.0145	1.06401

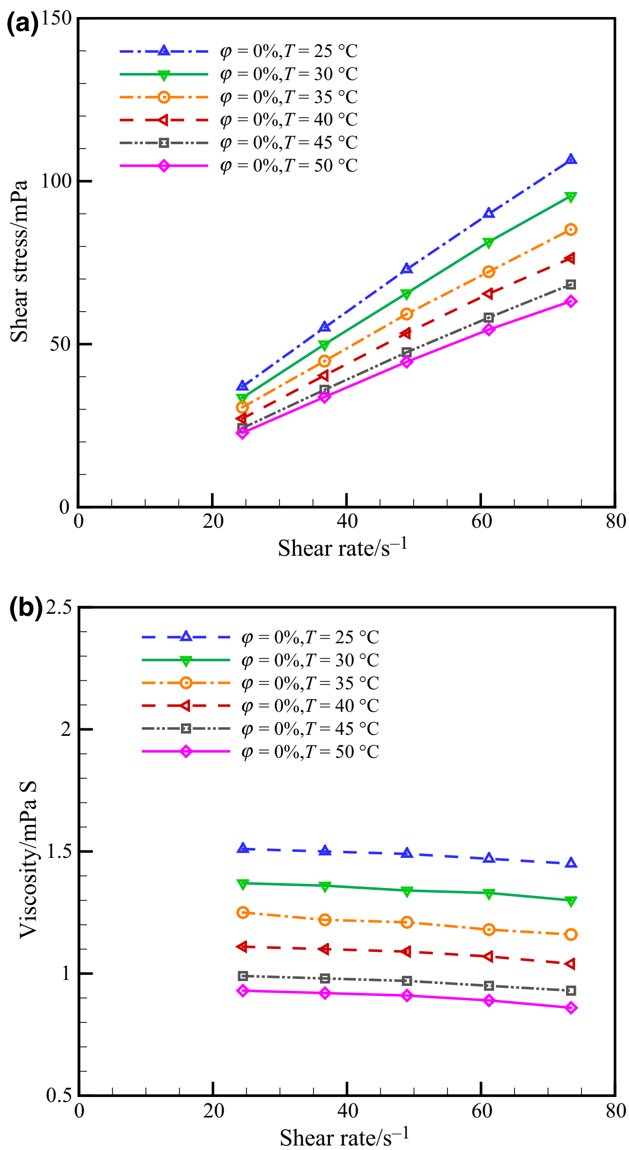

Fig. 4 **a** Shear stress versus shear rate at different temperatures at $\varphi = 0$, **b** viscosity versus shear rate at different temperatures at $\varphi = 0$

temperature. Table 4 shows a sample of measurements in a volume fraction of 0.25% and a temperature of 35 °C.

Calculation of error value

In order to validate the experiment, the Brookfield viscometer should be calibrated before use. The material used in the Brookfield viscometer is Silicon. In the initial experiments performed to determine the viscosity of the silicon sample at 25 °C, it was found that the measured viscosity is equal to the viscosity on the sample material (484 mPs). This match shows that the viscometer is calibrated. In Table 5, the values of the whole range and error are shown for the volume fraction of 0.625%, the temperature of 25 °C, and in different revolutions.

Investigating the rheological behavior of nanofluid

Base fluid

First, by measuring the viscosity of the base fluid in different revolutions of the viscometer according to Table 6, the rheological behavior of the base fluid is evaluated at 25 °C. The conversion factor of shear rate from rpm to s^{-1} for the applied spindle is equal to 1.223.

Figure 4a shows the shear stress versus shear rate at different temperature at $\varphi = 0$ and Fig. 4b shows the viscosity versus shear rate at different temperature at $\varphi = 0$. Figure 4 clearly shows that in this study, the base fluid has a Newtonian behavior. As shown in Fig. 4, no change occurred in the base fluid's rheological behavior. It can also be observed that by decreasing temperature and increasing the shear rate, the apparent viscosity is constant.

The nanofluid sample with $\varphi = 0.0625\%$

By measuring the nanofluid viscosity in different revolutions according to Table 7 at 45 °C, the rheological behavior of the nanofluid is evaluated. Figure 5a shows the shear stress versus shear rate at different temperature at $\varphi = 0.0625\%$, and Fig. 5b shows the viscosity versus shear rate at different temperature at $\varphi = 0.0625\%$. Figure 5 clearly shows that in this study, nanofluid has a

Table 7 The value of nanofluid viscosity in different revolutions of viscometer and corresponding shear stress at 45 °C and $\varphi = 0.0625\%$

Temperature/°C	Concentration/%	Shear rate		Viscosity		Shear stress/dyne cm^{-2}
		rpm	s^{-1}	cP	Poise	
45	0.0625	20	24.46	1.22	0.0122	0.2984
		30	36.69	1.21	0.0121	0.4439
		40	48.92	1.19	0.0119	0.5821
		50	61.15	1.17	0.0117	0.7154
		60	73.38	1.14	0.0114	0.8356

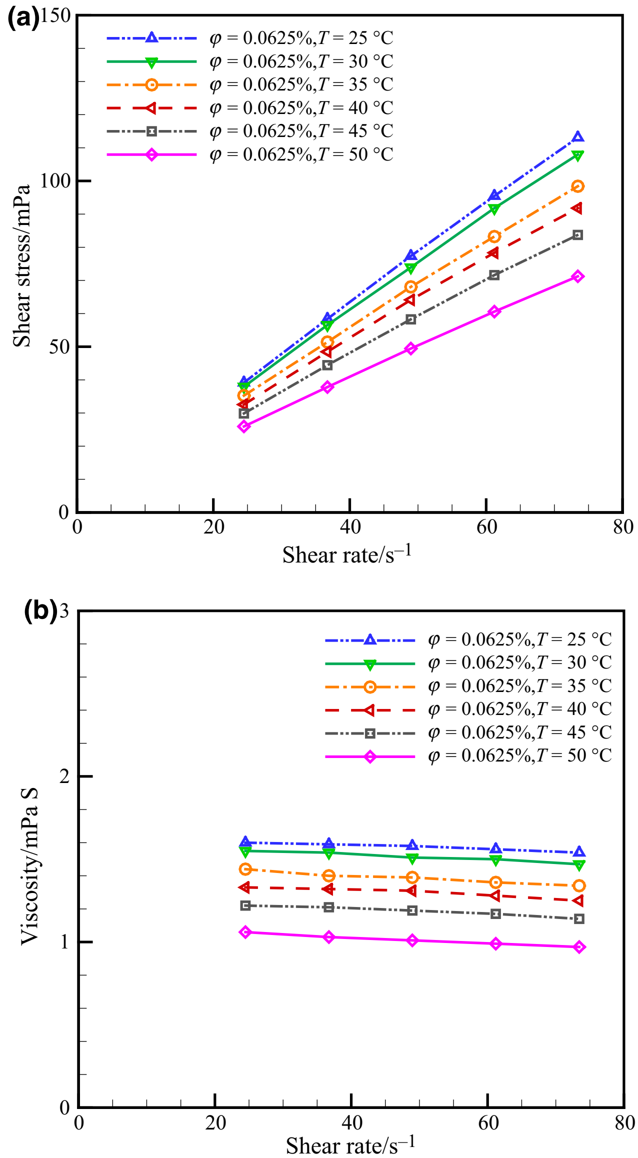

Fig. 5 **a** Shear stress versus shear rate at different temperatures at $\varphi = 0.0625\%$, **b** viscosity versus shear rate at different temperatures at $\varphi = 0.0625\%$

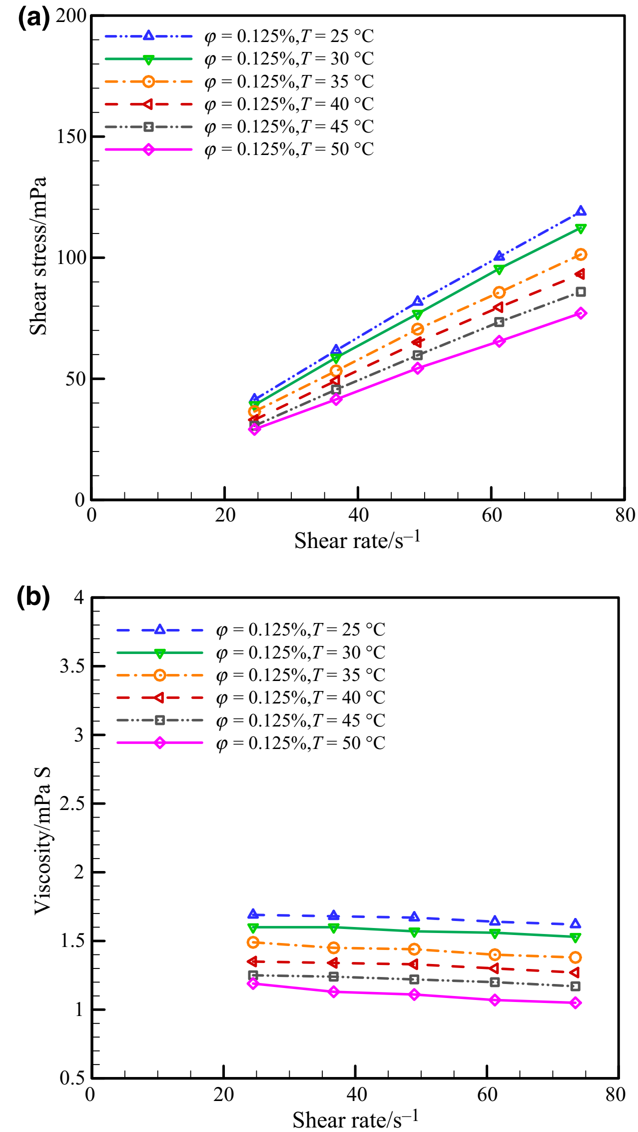

Fig. 6 **a** Shear stress versus shear rate at different temperatures at $\varphi = 0.125\%$, **b** viscosity versus shear rate at different temperatures at $\varphi = 0.125\%$

Newtonian behavior. As can be seen in Fig. 5, by adding a small amount of solid nanoparticles to the base fluid, the fluid's rheological behavior was not changed. It can also be seen that by decreasing temperature and increasing the shear rate, the apparent viscosity is constant.

Table 8 The value of nanofluid viscosity in different revolutions of viscometer and corresponding shear stress at 45 °C and $\varphi = 0.125\%$

Temperature/°C	Concentration/%	Shear rate		Viscosity		Shear stress/dyne cm^{-2}
		rpm	s^{-1}	cP	Poise	
45	0.125	20	24.46	1.25	0.0125	0.30575
		30	36.69	1.24	0.0124	0.45495
		40	48.92	1.22	0.0122	0.59682
		50	61.15	1.20	0.0120	0.7338
		60	73.38	1.17	0.0117	0.85854

Table 9 The value of nanofluid viscosity in different revolutions of viscometer and corresponding shear stress at 45 °C and $\varphi = 0.25\%$

Temperature/°C	Concentration/%	Shear rate		Viscosity		Shear stress/dyne cm^{-2}
		rpm	s^{-1}	cP	Poise	
45	0.25	20	24.46	1.48	0.0148	0.362008
		30	36.69	1.45	0.0145	0.532005
		40	48.92	1.43	0.0143	0.699556
		50	61.15	1.40	0.0140	0.8561
		60	73.38	1.37	0.0137	0.10053

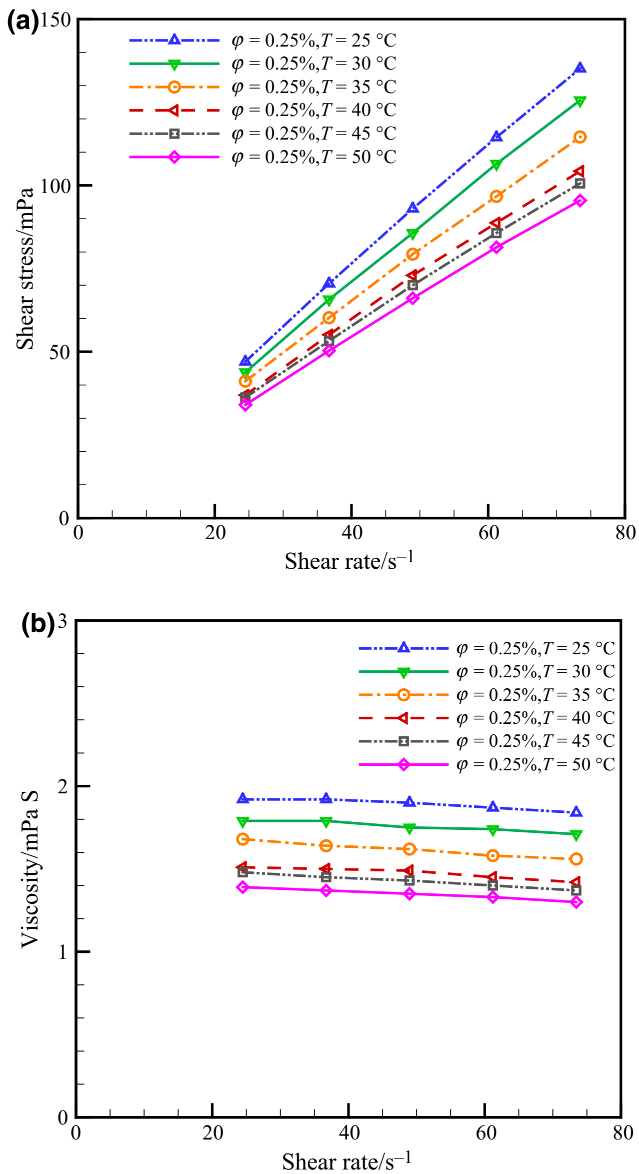

Fig. 7 **a** Shear stress versus shear rate at different temperatures at $\varphi = 0.25\%$, **b** viscosity versus shear rate at different temperatures at $\varphi = 0.25\%$

The nanofluid sample with φ = 0.125%

By measuring the nanofluid viscosity at different revolutions, according to Table 8, nanofluids rheological behavior is evaluated at 45 °C. Figure 6a shows the shear stress versus shear rate at different temperature at $\varphi = 0.125\%$, and Fig. 6b shows the viscosity versus shear rate at different temperature at $\varphi = 0.125\%$. Figure 6 clearly shows that in this study, the nanofluid has a Newtonian behavior.

The nanofluid sample with φ = 0.25%

By measuring the nanofluid viscosity at different revolutions according to Table 9, nanofluid rheological behavior is evaluated at 45 °C. Figure 7a shows the shear stress versus shear rate at different temperature at $\varphi = 0.25\%$, and Fig. 7b shows the viscosity versus shear rate at different temperature at $\varphi = 0.25\%$. Figure 7 clearly shows that in this study, nanofluid has a Newtonian behavior.

The nanofluid sample with φ = 0. 5%

By measuring the nanofluid viscosity at different revolutions according to Table 10, nanofluid rheological behavior is evaluated at 45 °C. Figure 8a shows the shear stress versus shear rate at different temperature at $\varphi = 0.5\%$, and Fig. 8b shows the viscosity versus shear rate at different temperature at $\varphi = 0.5\%$. Figure 8 clearly shows that in this study, nanofluid has a Newtonian behavior.

The nanofluid sample with φ = 0. 75%

By measuring the nanofluid viscosity at different revolutions according to Table 11, nanofluid rheological behavior is evaluated at 45 °C. Figure 9a shows the shear stress versus shear rate at different temperature at $\varphi = 0.75\%$, and Fig. 9b shows the viscosity versus shear rate at different temperature at $\varphi = 0.75\%$.

Figure 9 clearly indicated that in this study, nanofluid showed a pseudoplastic non-Newtonian behavior (the present nanofluid $n < 1$), and follows the Power Law model shown in Eq. (2).

Table 10 The value of nanofluid viscosity in different revolutions of viscometer and corresponding shear stress at 45 °C and $\varphi = 0.5\%$

Temperature/°C	Concentration/%	Shear rate		Viscosity		Shear stress/dyne cm^{-2}
		rpm	s^{-1}	cP	Poise	
45	0.5	20	24.46	1.87	0.0187	0.457402
		30	36.69	1.85	0.0185	0.678765
		40	48.92	1.83	0.0183	0.895236
		50	61.15	1.80	0.0180	1.1007
		60	73.38	1.75	0.0175	1.28415

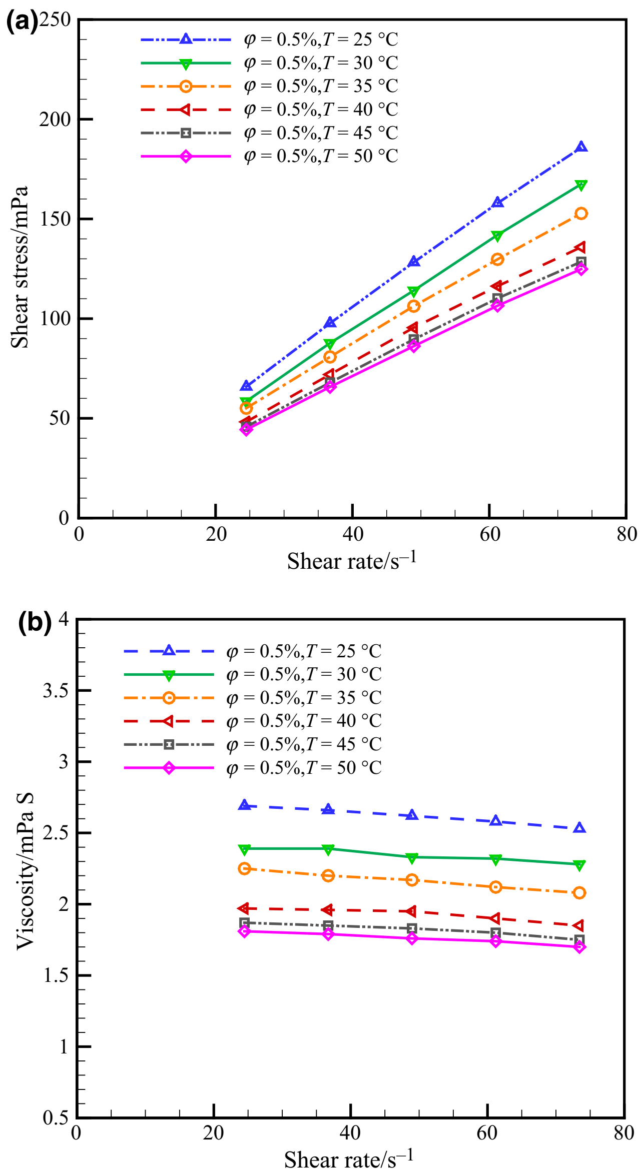

Fig. 8 **a** Shear stress versus shear rate at different temperatures at $\varphi = 0.5\%$, **b** viscosity versus shear rate at different temperatures at $\varphi = 0.5\%$

$$\tau_{yx} = m(\gamma_{yx})^n \quad (2)$$

Also apparent viscosity of Power Law fluid is calculated as follows:

$$\mu = \frac{\tau_{yx}}{\dot{\gamma}_{yx}} = m(\dot{\gamma}_{yx})^{n-1} \quad (3)$$

where τ is shear stress (Pa), $\dot{\gamma}$ is shear rate (s^{-1}), m is fluid strength index (Pa s^n), and n is the flow behavior index. As can be seen in Fig. 9, by adding a small amount of solid nanoparticles to the base fluid, the fluid's rheological behavior changed and the apparent viscosity becomes a function of the shear rate. It can also be seen that an increase occurs in apparent viscosity as the temperature is decreased, and apparent viscosity decreases with increasing shear rate.

The nanofluid sample with $\varphi = 1\%$

By measuring the nanofluid viscosity at different revolutions according to Table 12, nanofluid rheological behavior is evaluated at 45 °C. Figure 10a shows the shear stress versus shear rate at different temperature at $\varphi = 1\%$, and Fig. 10b shows the viscosity versus shear rate at different temperature at $\varphi = 1\%$.

Figure 10 clearly indicated that in this study, nanofluid showed a pseudoplastic non-Newtonian behavior (the present nanofluid $n < 1$). As can be seen in Fig. 10, by adding a small amount of solid nanoparticles to the base fluid, the fluid's rheological behavior changed and the apparent viscosity becomes a function of the shear rate. It can also be seen that an increase occurs in apparent viscosity as the temperature is decreased, and apparent viscosity decreases with increasing shear rate.

Effect of solid volume fraction

Figure 11 shows the effect of volume fraction on dynamic viscosity at different temperatures. As can be seen in Fig. 11, According to this figure, dynamic viscosity of fluid increases with increasing the volume fraction, whereas the diagram shows that the dynamic viscosity decreases with increasing temperature.

Table 11 The value of nanofluid viscosity in different revolutions of viscometer and corresponding shear stress at 45 °C and $\varphi = 0.75\%$

Temperature/°C	Concentration/%	Shear rate		Viscosity		Shear stress/dyne cm^{-2}
		rpm	s^{-1}	cP	Poise	
45	0.75	5	6.115	6.25	0.0625	0.382187
		10	12.23	5.13	0.0513	0.627399
		20	24.46	3.87	0.0387	0.946602
		30	36.69	3.26	0.0326	1.196094
		40	48.96	2.87	0.0287	1.404004

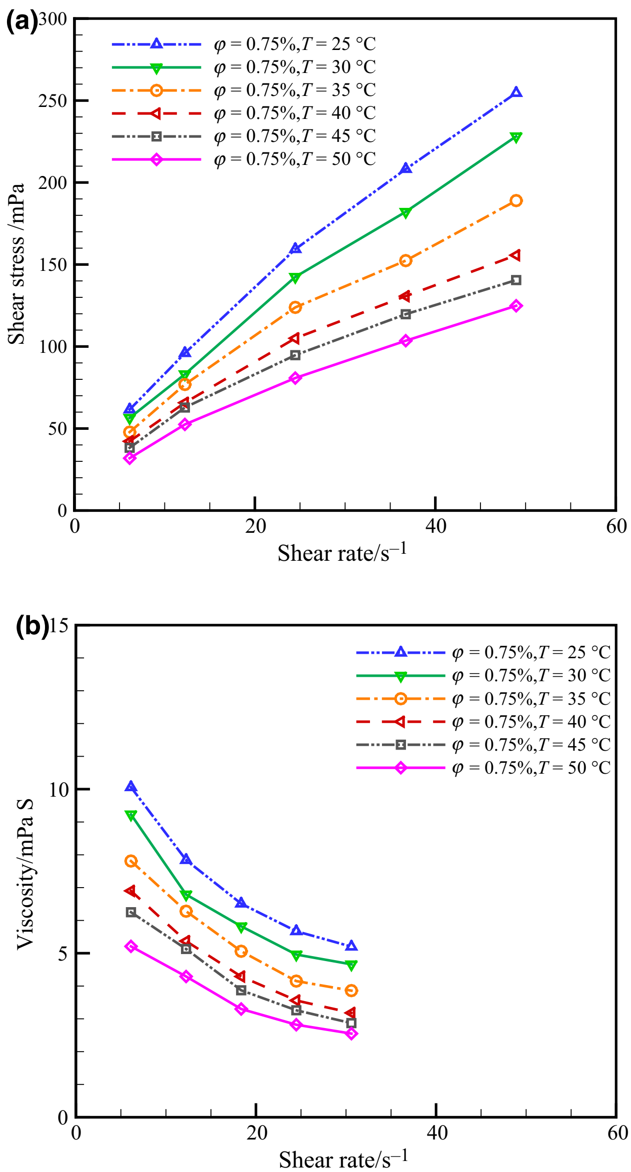

Fig. 9 **a** Shear stress versus shear rate at different temperatures at $\varphi = 0.75\%$, **b** viscosity versus shear rate at different temperatures at $\varphi = 0.75\%$

Reasons for justifying this phenomenon are as follows:

1. *Brownian motion* This random motion of nanoparticles in base fluid is one of the factors affecting the viscosity. This random motion occurs due to continuous collisions between nanoparticles and base fluid molecules.
2. When nanoparticles are added to base fluid, these nanomaterials are dispersed in base fluid and symmetrical and larger nanoclusters are formed due to van der Waals force between the nanoparticles and base fluid. These nanoclusters inhibit the movement of ethylene-glycol on one another, resulting in an increase in viscosity.
3. Since nanostructures have a super-high surface-to-volume ratio, qualities such as density are changed due to being nano, and floating forces and weight loose their importance due to their ultra-small size and super-low mass, and superficial and intermolecular forces play an important role.
4. The presence of nanomaterials in the base fluid causes an increase in intermolecular forces that increase viscosity.

Effect of temperature

Figure 12 shows the effect of temperature on dynamic viscosity in different volume fractions. As shown in Fig. 12, by comparing the changes in viscosity with changing the temperature in different volume fractions, it can be observed that the nanofluid viscosity decreases with increasing the temperature in a constant volume fraction.

Some reasons for justifying this phenomenon are as follows:

1. Viscosity is a property caused by intermolecular cohesive forces in liquids which changes with temperature change. Liquids' viscosity reduces with increasing the temperature. Molecules of liquids are under the influence of more energy at higher temperatures and

Table 12 The value of nanofluid viscosity in different revolutions of viscometer and corresponding shear stress at 45 °C and $\varphi = 1\%$

Temperature/°C	Concentration/%	Shear rate		Viscosity		Shear stress/dyne cm^{-2}
		rpm	s^{-1}	cP	Poise	
45	0.1	5	6.115	14.5	0.145	0.886675
		10	12.23	10.31	0.1031	1.260913
		20	18.345	7.98	0.0798	1.463931
		30	24.46	7.16	0.0716	1.751336
		40	30.575	6.54	0.0654	1.999605

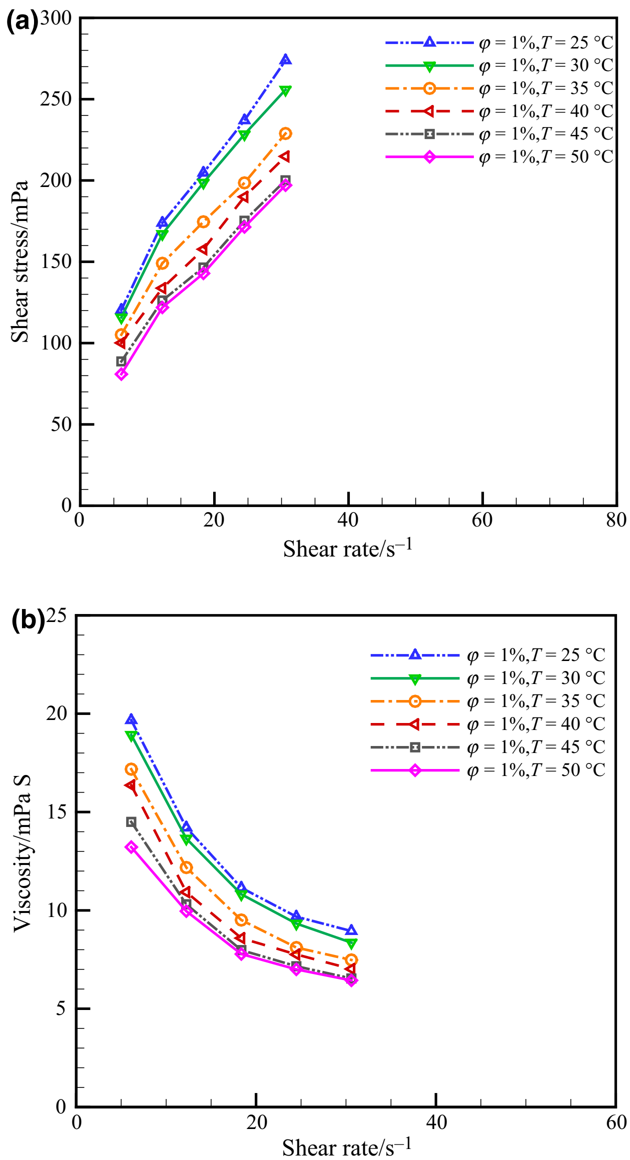

Fig. 10 **a** Shear stress versus shear rate at different temperatures at $\varphi = 1\%$, **b** viscosity versus shear rate at different temperatures at $\varphi = 1\%$

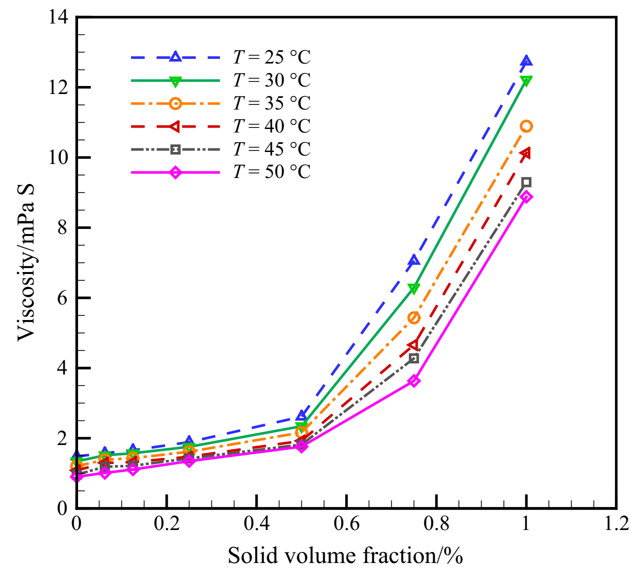

Fig. 11 Effect of volume fraction on dynamic viscosity at different temperatures

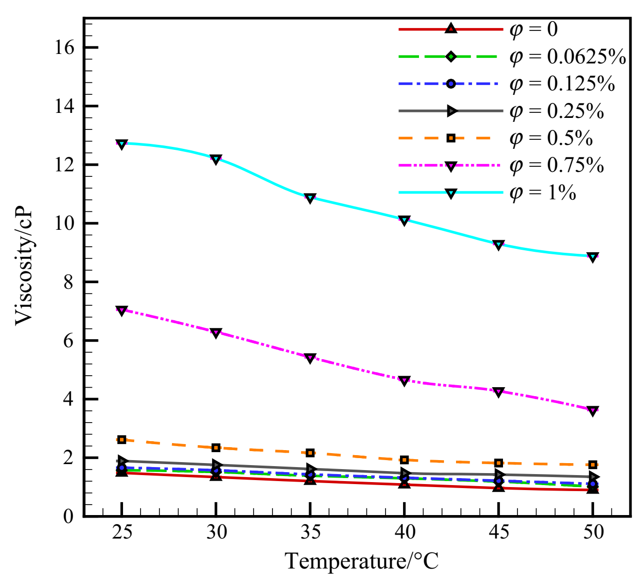

Fig. 12 Effect of temperature on dynamic viscosity in different solid volume fractions

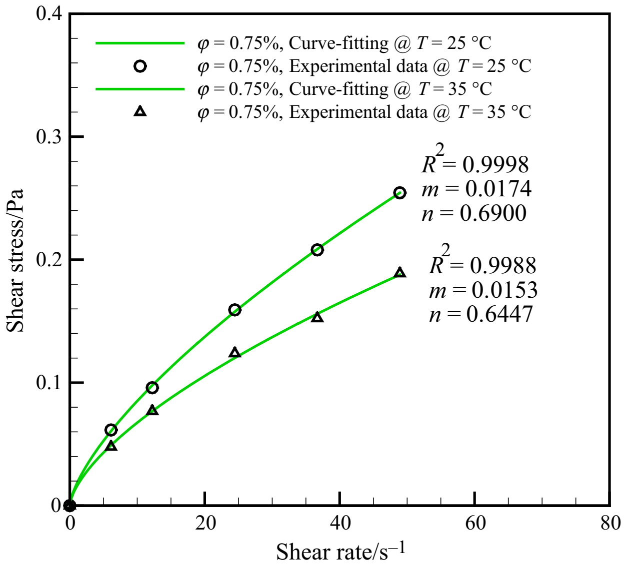

Fig. 13 Curve fitting to laboratory data in volume fraction of 0.75%

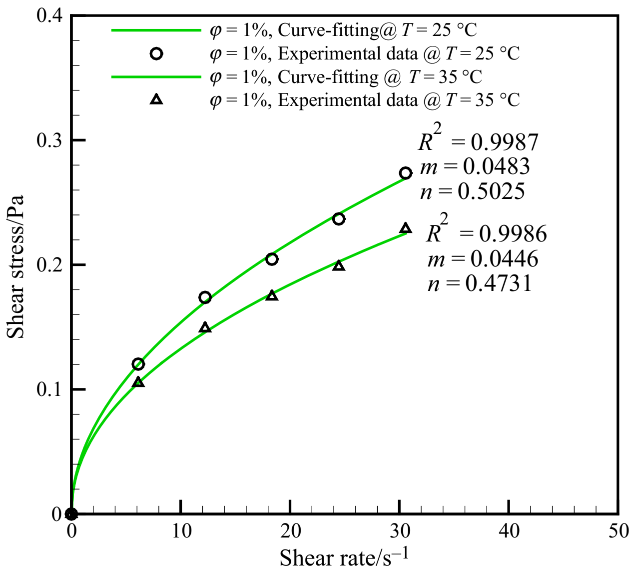

Fig. 14 Curve fitting to laboratory data in volume fraction of 1%

can overcome the intermolecular cohesive forces. As a result, energetic molecules move more easily. Reduction in intermolecular forces due to an increase in temperature reduces the resistance to flow. As a result, Newtonian nanofluid viscosity decreases with increasing temperature.

2. The effect of the nanoparticle's Brownian motion with increasing temperature on nanofluid viscosity is also justifiable.
3. As the temperature increases, the intermolecular distance between nanoparticles and base fluid increased, resulting in reduced flow resistance and viscosity.

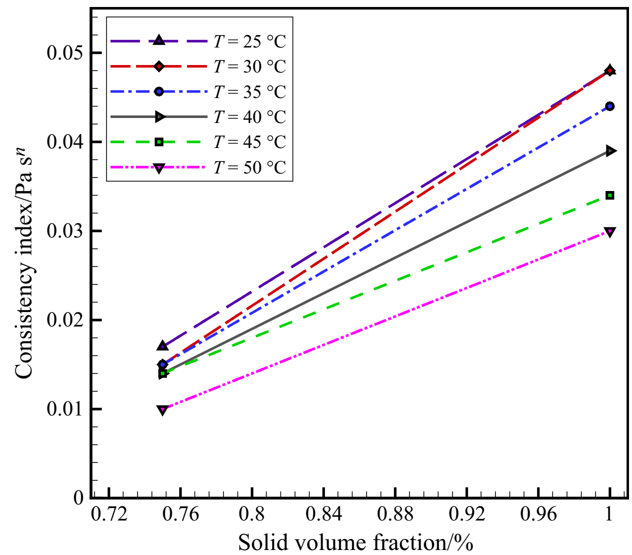

Fig. 15 Fluid strength changes versus solid volume fractions at different temperatures

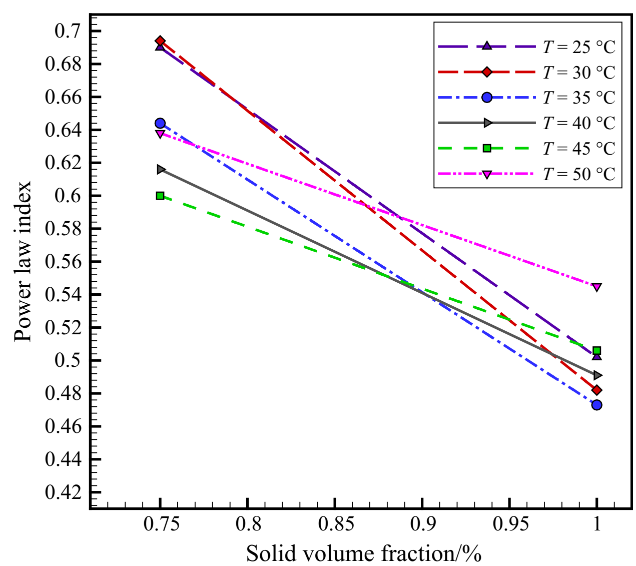

Fig. 16 Flow index changes relative to different volume fractions and temperatures

Curve fitting

As seen in Figs. 4–8, the shear stress is a linear function of the shear rate (Newtonian fluid). In Newtonian fluids, n is equal to 1 and m is not defined, but it is observed in Figs. 9 and 10 that the shear stress is a nonlinear function of the shear rate (non-Newtonian fluid), and in non-Newtonian fluids, n is less than 1 and m is obtained. By analyzing these figures, it can be observed that shear stress is also a function of temperature and volume fraction; therefore, by fitting the curve and using Eqs. 2–3, the values of m, n and R^2 can be achieved for each temperature and volume

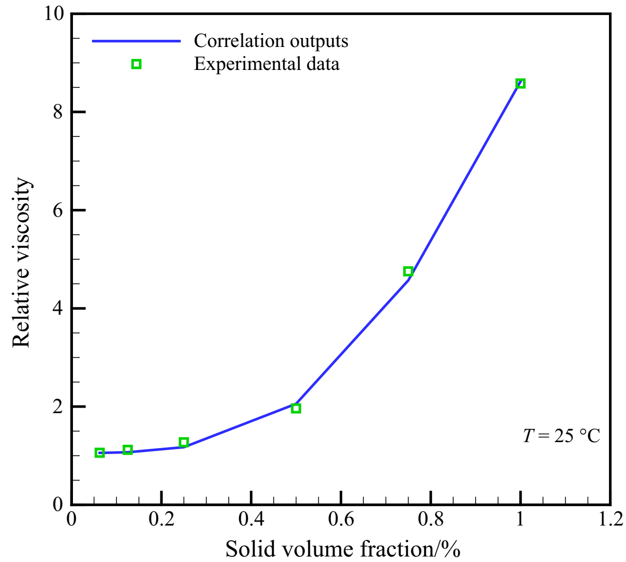

Fig. 17 Comparison between laboratory results and the extracted mathematical equation at 25 °C

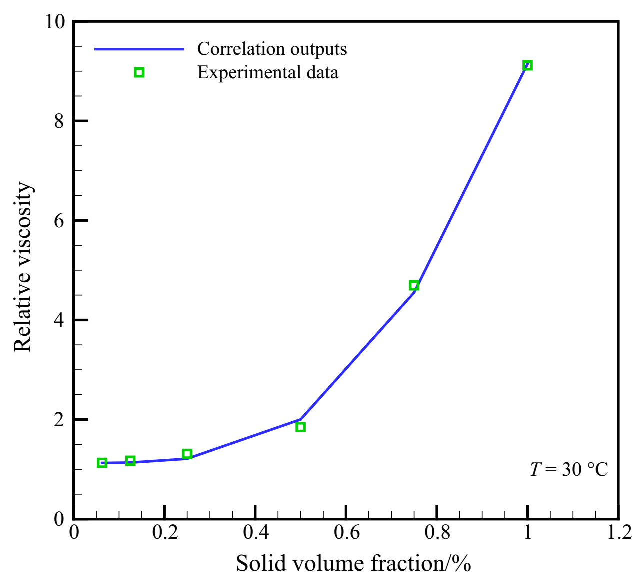

Fig. 18 Comparison between laboratory results and the extracted mathematical equation at 30 °C

fraction (R^2 is coefficient which is an indicator of the relationship between the variables. R^2 is an appropriate criterion for determining the correlation between the two quantitative variables. It should be noted that the closer this coefficient to 1, the greater the correlation of the two variables). Examples of fitting a power law curve to experimental data in Figs. 13 and 14 are provided. As seen in these figures, there is a great deal of accuracy in this fitting. Curve fitting was performed for each nanofluid sample at different temperatures, and the results are provided in Figs. 15 and 16. Since from volume fraction of

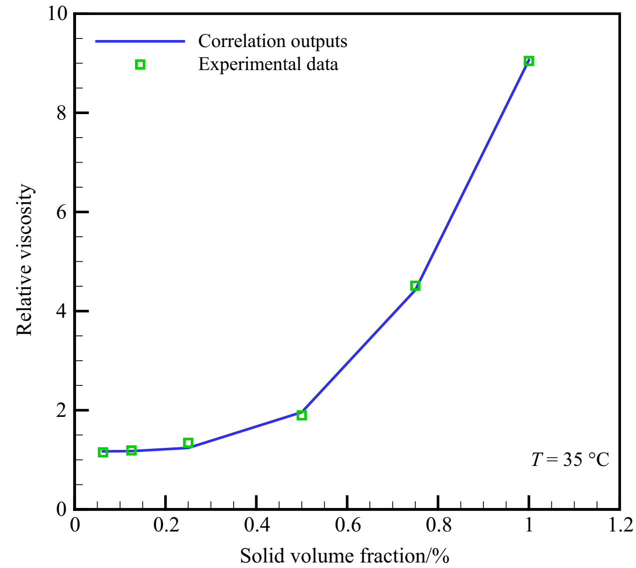

Fig. 19 Comparison between laboratory results and the extracted mathematical equation at 35 °C

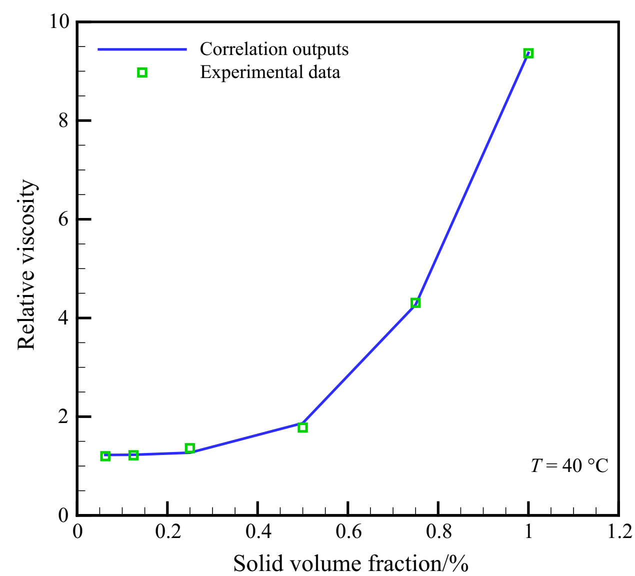

Fig. 20 Comparison between laboratory results and the extracted mathematical equation at 40 °C

0.75% onward, the fluid was non-Newtonian, it can be seen from the observation of m in Fig. 15 that m increases with increasing volume fraction and decreases with increasing temperature. In fact, according to Eqs. 2 and 3, the apparent viscosity is directly related to m; so the result shows a decrease in nanofluid viscosity with temperature and its increase with volume fraction. As shown in Fig. 16, the values of n are always less than 1, which means that with increasing the shear rate, the apparent viscosity decreases. Also, the value of n decreases with increasing

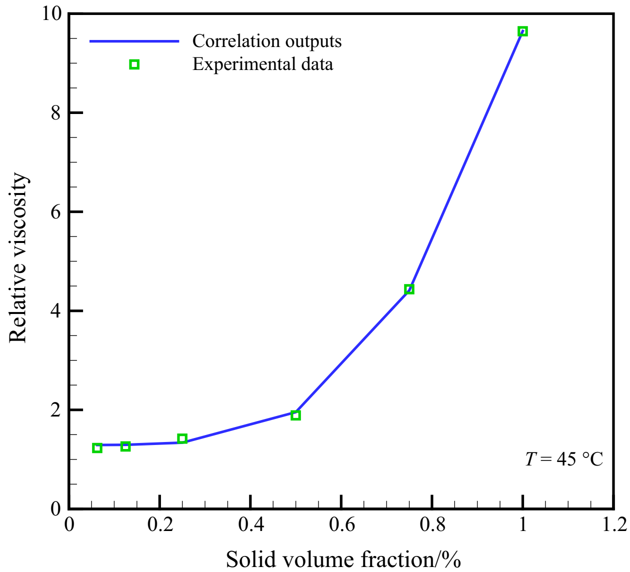

Fig. 21 Comparison between laboratory results and the extracted mathematical equation at 45 °C

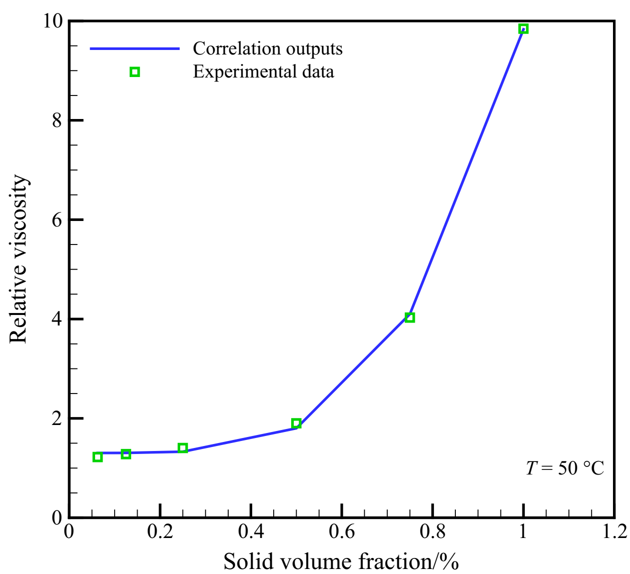

Fig. 22 Comparison between laboratory results and the extracted mathematical equation at 50 °C

volume fraction; it means that the fluid behavior is getting farther from Newtonian state.

Suggested relation

By fitting the diagram curve in SigmaPlot 12.3, relations with the coefficients for each temperature (6 temperatures in the experiment range) were extracted. In these equations, φ is the volume fraction of the nanoparticles to the base fluid, μ_{bf} is the viscosity of the base fluid, μ_{nf} is the

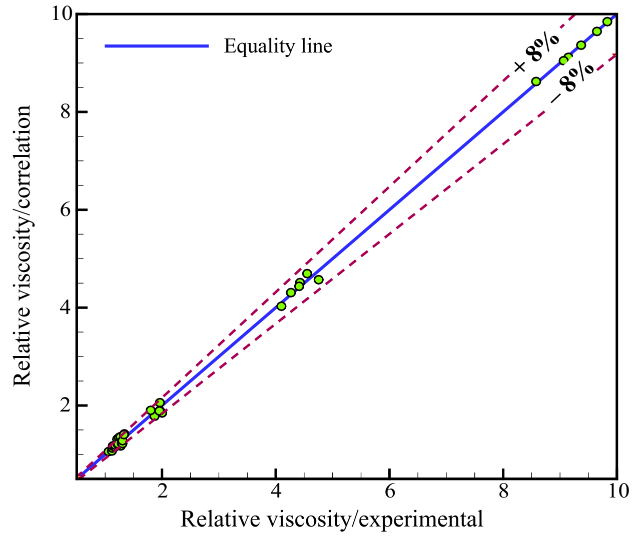

Fig. 23 Margin of deviation for all data

nanofluid viscosity, and μ_{r} is the relative viscosity (the ratio of nanofluid viscosity to fluid viscosity).

The equation of relative viscosity at a temperature of 25 °C:

$$\mu_{\mathrm{r}} = \frac{\mu_{\mathrm{nf}}}{\mu_{\mathrm{bf}}} = 1.0560 + \left(8.5662\varphi^{3.0971}\right) + \left(\varphi^{8.5662}\right)^{5} \tag{4}$$

The equation of relative viscosity at a temperature of 30 °C:

$$\mu_{\mathrm{r}} = \frac{\mu_{\mathrm{nf}}}{\mu_{\mathrm{bf}}} = 1.1262 + \left(9.0211\varphi^{3.3657}\right) + \left(\varphi^{9.0211}\right)^{5} \tag{5}$$

The equation of relative viscosity at a temperature of 35 °C:

$$\mu_{\mathrm{r}} = \frac{\mu_{\mathrm{nf}}}{\mu_{\mathrm{bf}}} = 1.1699 + \left(8.8939\varphi^{3.4919}\right) + \left(\varphi^{8.8939}\right)^{5} \tag{6}$$

The equation of relative viscosity at a temperature of 40 °C:

$$\mu_{\mathrm{r}} = \frac{\mu_{\mathrm{nf}}}{\mu_{\mathrm{bf}}} = 1.2245 + \left(9.1468\varphi^{3.8255}\right) + \left(\varphi^{9.1468}\right)^{5} \tag{7}$$

The equation of relative viscosity at a temperature of 45 °C:

$$\mu_{\mathrm{r}} = \frac{\mu_{\mathrm{nf}}}{\mu_{\mathrm{bf}}} = 1.2913 + \left(9.3580\varphi^{3.8180}\right) + \left(\varphi^{9.3580}\right)^{5} \tag{8}$$

The equation of relative viscosity at a temperature of 50 °C:

$$\mu_{\mathrm{r}} = \frac{\mu_{\mathrm{nf}}}{\mu_{\mathrm{bf}}} = 1.3038 + \left(9.5283\varphi^{4.2613}\right) + \left(\varphi^{9.5283}\right)^{5}. \tag{9}$$

Comparison of the experimental results and the data obtained from the extracted relation

Figures 17–22 represent the comparison of the experimental results and the data obtained from the extracted relation. It can be concluded that the obtained mathematical equation is a suitable predictor model for estimating the desired nanofluid viscosity, which is in the range of volume fractions and determined temperatures consistent with laboratory results.

Margin of deviation

The margin of deviation between laboratory results and extracted experimental equations can be obtained using following equation:

$$\text{Dev} = \left[\frac{\mu_{\text{Exp}} - \mu_{\text{Pred}}}{\mu_{\text{Exp}}}\right] \times 100\% \quad (10)$$

The Rsqr value of each mathematical equation is close to 0.997, which is satisfactory for equations obtained from curve fitting operation (Fig. 23). This figure also shows the computed margin of deviation between laboratory results and experimental equations in different volume fractions and temperatures. According to the figure, the margin of deviation is equal to 8%.

Conclusions

In this paper, experimental investigation of the effects of solid volume concentration and temperature on dynamic viscosity of the hybrid nanofluid of multi-walled carbon nanotubes and aluminum oxide in a mixture of water (80%) and ethylene-glycol (20%) has been presented. The nanofluid was prepared with solid volume fractions of 0.0625, 0.125, 0.25, 0.5, 0.75 and 1%, and experiments were performed in the temperature range of 25–50 °C. Following results were deduced:

- The nanofluid viscosity decreases with increasing the temperature in a constant solid volume fraction.
- Dynamic viscosity of fluid increases with increasing the solid volume fraction.
- For $\varphi = 0.0625$, 0.125, 0.25 and 0.5% nanofluid showed a Newtonian behavior.
- For $\varphi = 0.75\%$ and $\varphi = 1\%$ nanofluid showed a pseudoplastic non-Newtonian behavior.
- The results also revealed that the apparent viscosity generally increases with an increase in the solid volume fraction.
- According to the experimental results a new mathematical correlation was presented to predict the nanofluid viscosity, which is in the range of solid volume fractions and determined temperatures and has a good accuracy.

The extension of this paper according our previous works about nanofluid [35–51] affords engineers a good option for micro- and nanoscale investigation.

References

1. Rezaei M, Azimian AR, Toghraie D. The surface charge density effect on the electro-osmotic flow in a nanochannel: a molecular dynamics study. Heat Mass Transf. 2015;51(5):661–70.
2. Dardan E, Afrand M, Isfahani AM. Effect of suspending hybrid nano-additives on rheological behavior of engine oil and pumping power. Appl Therm Eng. 2016;109:524–34.
3. Afrand M, Najafabadi KN, Sina N, Safaei MR, Kherbeet AS, Wongwises S, Dahari M. Prediction of dynamic viscosity of a hybrid nano-lubricant by an optimal artificial neural network. Int Commun Heat Mass Transf. 2016;76:209–14.
4. Vafaei M, Afrand M, Sina N, Kalbasi R, Sourani F, Teimouri H. Evaluation of thermal conductivity of MgO–MWCNTs/EG hybrid nanofluids based on experimental data by selecting optimal artificial neural networks. Physica E. 2017;85:90–6.
5. Afrand M. Experimental study on thermal conductivity of ethylene glycol containing hybrid nano-additives and development of a new correlation. Appl Therm Eng. 2017;110:1111–9.
6. Rezaei M, Azimian AR, Toghraie D. Molecular dynamics study of an electro-kinetic fluid transport in a charged nanochannel based on the role of the stern layer. Physica A: Stat Mech Appl. 2015;426:25–34.
7. Afrand M, Nadooshan AA, Hassani M, Yarmand H, Dahari M. Predicting the viscosity of multi-walled carbon nanotubes/water nanofluid by developing an optimal artificial neural network based on experimental data. Int Commun Heat Mass Transf. 2016;77:49–53.
8. Afrand M, Farahat S, Nezhad AH, Sheikhzadeh GA, Sarhaddi F. Numerical simulation of electrically conducting fluid flow and free convective heat transfer in an annulus on applying a magnetic field. Heat Transf Res. 2014;45:749–66.
9. Gravndyan Q, Akbari OA, Toghraie D, Marzban A, Mashayekhi R, Karimi R, Pourfattah F. The effect of aspect ratios of rib on the heat transfer and laminar water/TiO 2 nanofluid flow in a two-dimensional rectangular microchannel. J Mol Liq. 2017;236:254–265. https://doi.org/10.1007/s10973-017-6711-8
10. Shahsavani E, Afrand M, Kalbasi R. Using experimental data to estimate the heat transfer and pressure drop of non-Newtonian nanofluid flow through a circular tube: applicable for use in heat exchangers. Appl Therm Eng. 2018;129:1573–81.
11. Mahmoodi M, Esfe MH, Akbari M, Karimipour A, Afrand M. Magneto-natural convection in square cavities with a source-sink pair on different walls, nt. J Appl Electromagn Mech. 2015;47:21–32.
12. Afrand M, Toghraie D, Karimipour A, Wongwises S. A numerical study of natural convection in a vertical annulus filled with gallium in the presence of magnetic field. J Magn Magn Mater. 2017;430:22–8.
13. Tohidi M, Toghraie D. The effect of geometrical parameters, roughness and the number of nanoparticles on the self-diffusion coefficient in Couette flow in a nanochannel by using of molecular dynamics simulation. Physica B: Condensed Matt. 2017;518:20–32.

14. Shamsi MR, Akbari OA, Marzban A, Toghraie D, Mashayekhi R. Increasing heat transfer of non-Newtonian nanofluid in rectangular microchannel with triangular ribs. Physica E: Low-dimensional Syst Nanostruct. 2017;93:167–178.
15. Afrand M. Using a magnetic field to reduce natural convection in a vertical cylindrical annulus. Int J Therm Sci. 2017;118:12–23.
16. Afrand M, Farahat S, Nezhad AH, AliSheikhzadeh G, Sarhaddi F. 3-D numerical investigation of natural convection in a tilted cylindrical annulus containing molten potassium and controlling it using various magnetic fields. Int J Appl Electromagn Mech. 2014;46(4):809–21.
17. Teimouri H, Afrand M, Sina N, Karimipour A, Isfahani AHM. Natural convection of liquid metal in a horizontal cylindrical annulus under radial magnetic field. Int J Appl Electromagn Mech. 2015;49:453–61.
18. Namburu PK, Kulkarni DP, Misra D, Das DK. Viscosity of copper oxide nanoparticles dispersed in ethylene glycol and water mixture. Exp Therm Fluid Sci. 2007;32(2):397–402.
19. Chen H, Ding Y, Tan C. Rheological behaviour of nanofluids. New J Phys. 2007;9(10):367.
20. Chen H, Ding Y, Lapkin A. Rheological behaviour of nanofluids containing tube/rod-like nanoparticles. Powder Technol. 2009;194(1):132–41.
21. Masoumi N, Sohrabi N, Behzadmehr A. A new model for calculating the effective viscosity of nanofluids. J Phys D Appl Phys. 2009;42(5):1–6.
22. Fedele L, Colla L. Bobbo S Viscosity and thermal conductivity measurements of water-based nanofluids containing titanium oxide nanoparticles. Int J Refrig. 2012;35(5):1359–66.
23. Mahbubul IM, Saidur R, Amalina MA. Investigation of viscosity of R123-TiO_2 nanorefrigerant. Int J Mech Mater Eng. 2012;7(2):146–51.
24. Mishra PC, Mukherjee S, Nayak SK, Panda A. A brief review on viscosity of nanofluids. Int Nano Lett. 2014;4(4):109–20.
25. Anoop K, Sadr R, Al-Jubouri M, Amani M. Rheology of mineral oil-SiO_2 nanofluids at high pressure and high temperatures. Int J Therm Sci. 2014;77:108–15.
26. Nwosu PN, Meyer J, Sharifpur M. Review and parametric investigation into nanofluid viscosity models. J Nanotechnol Eng Med. 2007;32(2):397–402.
27. Li X, Zou C, Wang T, Lei X. Rheological behavior of ethylene glycol-based SiC nanofluids. Int J Heat Mass Transf. 2015;84:925–30.
28. Ghozatloo A, Azimi MS, Shariaty-Niassar M, Morad Rashidi A. Investigation of nanoparticles morphology on viscosity of nanofluids and new correlation for prediction. J Nanostruct. 2015;5:161–8.
29. Etaig S, Hasan R, Perera N. Investigation of a new effective viscosity model for nanofluids. Proc Eng. 2016;157:404–13.
30. Issa RJ. Effect of nanoparticles size and concentration on thermal and rheological properties of Al_2O_3–water nanofluids. 2016; Paper No. ENFHT 101.
31. Auriemma M, Iazzetta A. Viscosity of alumina water-based nanofluids modeling by artificial neural network. Indian J Sci Technol. 2017. https://doi.org/10.17485/ijst/2016/v9i48/91743.
32. Kavosh M. The viscosity study of CuO nanofluid based on propylene glycol. Int J Math Phys Sci Res. 2016;4(1):96–103.
33. Zhao N, Li Z. Viscosity prediction of different ethylene glycol/water based nanofluids using a RBF neural network. Appl Sci. 2017;7(4):409.
34. Esfe MH. The investigation of effects of temperature and nanoparticles volume fraction on the viscosity of copper oxide–ethylene glycol nanofluids. Period Polytech Chem Eng. 2018. https://doi.org/10.3311/PPch.9741.
35. Esfe MH, Saedodin S, Bahiraei M, Toghraie D, Mahian O, Wongwises S. Thermal conductivity modeling of MgO/EG nanofluids using experimental data and artificial neural network. J Therm Anal Calorim. 2014;118(1):287–94.
36. Zarringhalam M, Karimipour A, Toghraie D. Experimental study of the effect of solid volume fraction and Reynolds number on heat transfer coefficient and pressure drop of CuO–water nanofluid. Exp Therm Fluid Sci. 2016;76:342–51.
37. Esfe MH, Akbari M, Semiromi DT, Karimiopour A, Afrand M. Effect of nanofluid variable properties on mixed convection flow and heat transfer in an inclined two-sided lid-driven cavity with sinusoidal heating on sidewalls. Heat Transf Res. 2014;45(5):409–32.
38. Afrand M, Toghraie D, Ruhani B. Effects of temperature and nanoparticles concentration on rheological behavior of Fe_3O_4–Ag/EG hybrid nanofluid: an experimental study. Exp Therm Fluid Sci. 2016;77:38–44.
39. Esfe MH, Yan WM, Afrand M, Sarraf M, Toghraie D, Dahari M. Estimation of thermal conductivity of Al_2O_3/water (40%)–ethylene glycol (60%) by artificial neural network and correlation using experimental data. Int Commun Heat Mass Transf. 2016;74:125–8.
40. Toghraie D, Chaharsoghi VA, Afrand M. Measurement of thermal conductivity of ZnO–TiO_2/EG hybrid nanofluid. J Therm Anal Calorim. 2016;125(1):527–35.
41. Toghraie D, Alempour SM, Afrand M. Experimental determination of viscosity of water based magnetite nanofluid for application in heating and cooling systems. J Magn Magn Mater. 2016;417:243–8.
42. Esfe MH, Saedodin S, Wongwises S, Toghraie D. An experimental study on the effect of diameter on thermal conductivity and dynamic viscosity of Fe/water nanofluids. J Therm Anal Calorim. 2015;119(3):1817–24.
43. Esfe MH, Afrand M, Gharehkhani S, Rostamian H, Toghraie D, Dahari M. An experimental study on viscosity of alumina-engine oil: effects of temperature and nanoparticles concentration. Int Commun Heat Mass Transf. 2016;76:202–8.
44. Esfe MH, Afrand M, Yan WM, Yarmand H, Toghraie D, Dahari M. Effects of temperature and concentration on rheological behavior of MWCNTs/SiO_2 (20–80)-SAE40 hybrid nano-lubricant. Int Commun Heat Mass Transf. 2016;76:133–8.
45. Esfe MH, Ahangar MRH, Rejvani M, Toghraie D, Hajmohammad MH. Designing an artificial neural network to predict dynamic viscosity of aqueous nanofluid of TiO_2 using experimental data. Int Commun Heat Mass Transf. 2016;75:192–6.
46. Afrand M, Toghraie D, Sina N. Experimental study on thermal conductivity of water-based Fe_3O_4 nanofluid: development of a new correlation and modeled by artificial neural network. Int Commun Heat Mass Transf. 2016;75:262–9.
47. Esfahani MA, Toghraie D. Experimental investigation for developing a new model for the thermal conductivity of silica/water–ethylene glycol (40%–60%) nanofluid at different temperatures and solid volume fractions. J Mol Liq. 2017;232:105–12.
48. Esfe MH, Afrand M, Rostamian SH, Toghraie D. Examination of rheological behavior of MWCNTs/ZnO-SAE40 hybrid nano-lubricants under various temperatures and solid volume fractions. Exp Therm Fluid Sci. 2017;80:384–90.
49. Esfe MH, Rostamian H, Toghraie D, Yan WM. Using artificial neural network to predict thermal conductivity of ethylene glycol with alumina nanoparticle. J Therm Anal Calorim. 2016;126(2):643–8.
50. Zadkhast M, Toghraie D, Karimipour A. Developing a new correlation to estimate the thermal conductivity of MWCNT-CuO/water hybrid nanofluid via an experimental investigation. J Therm Anal Calorim. 2017;129:859–67.
51. Esfe MH, Hajmohammad H, Toghraie D, Rostamian H, Mahian O, Wongwises S. Multi-objective optimization of nanofluid flow in double tube heat exchangers for applications in energy systems. Energy. 2017;137:160–71.